

Letters

Direct Measurement of the Counterion Distribution within Swollen Polyelectrolyte Films

Vivek M. Prabhu,^{*,†} Bryan D. Vogt,[†] Wen-li Wu,[†] Jack F. Douglas,[†] Eric K. Lin,[†]
Sushil K. Satija,[‡] Dario L. Goldfarb,[§] and Hiroshi Ito^{||}

*Polymers Division, Center for Neutron Research, National Institute of Standards and
Technology, Gaithersburg, Maryland 20899, IBM T. J. Watson Research Center, Yorktown
Heights, New York 10598, and IBM Almaden Research Center, San Jose, California 95120*

Received February 7, 2005. In Final Form: May 31, 2005

The depth profile of the counterion concentration within thin polyelectrolyte films was measured *in situ* using contrast variant specular neutron reflectivity to characterize the initial swelling stage of the film dissolution. We find substantial counterion depletion near the substrate and enrichment near the periphery of the film extending into the solution. These observations challenge our understanding of the charge distribution in polyelectrolyte films and are important for understanding film dissolution in medical and technological applications.

1. Introduction

The transformation of a solid-like film into a solution upon exposure to a miscible solvent is a complex process involving sluggish kinetic pathways associated with the slow transport of the liquid into the film and the evolution of the thermodynamic driving forces during the course of the dissolution process. In complex materials such as polymers, this process occurs in stages from the transformation of the glassy or crystalline film into a swollen gel-like state, followed at much longer times by the final dissolution of the film.^{1–3} Recent advances in measurement have allowed a better characterization of this technologi-

cally important process. The specific dissolution mechanism can be tailored to different applications, as the controlled release of drugs from water soluble polymer matrices in the pharmaceutical industry⁴ and in the microelectronics industry where the dissolution of one component enables lithographic pattern formation.⁵ Control over component release rates or lithographic performance in these medical and fabrication applications, respectively, is strongly dependent upon the initial stages of polymer dissolution.

Dissolving polyelectrolyte films exhibit additional complexities in their dissolution dynamics over uncharged polymer films. Interfacial charge density, the dielectric constant of the medium, ionic strength, and valence influence the phase behavior of charged polymer and colloidal solutions thus affecting their dissolution behavior. Some of the physics necessary for describing such films has been considered in recent measurements on model synthetic⁶ and biological⁷ polyelectrolyte brushes. How-

* To whom correspondence should be addressed. Fax: 301-975-3928. E-mail: vprabhu@nist.gov.

[†] Polymers Division, NIST.

[‡] Center for Neutron Research, NIST.

[§] IBM T. J. Watson Research Center.

^{||} IBM Almaden Research Center.

(1) Hinsberg, W.; Houle, F. A.; Lee, S. W.; Ito, H.; Kanazawa, K. *Macromolecules* **2005**, *38* (5), 1882–1898.

(2) Hinsberg, W. D.; Houle, F. A.; Ito, H.; Kanazawa, K.; Lee, S. W. *Proceedings of the 13th International Conference on Photopolymers, Advances in Imaging Materials and Processes*, RETEC **2003**, 193–209.

(3) Ueberreiter, K. *Diffusion in Polymers*; Academic Press: New York, 1968; pp 219–257.

(4) Siepman, J.; Gopferich, A. *Adv. Drug Delivery Rev.* **2001**, *48* (2–3), 229–247.

(5) Ito, H. *Adv. Polym. Sci.* **2005**, *172*, 37–245.

(6) Biesalski, M.; Johannsmann, D.; Rühle, J. *J. Chem. Phys.* **2002**, *117* (10), 4988–4994.

ever, these studies do not address the important matter of the counterion distribution, which is expected to influence the course of the dissolution process.

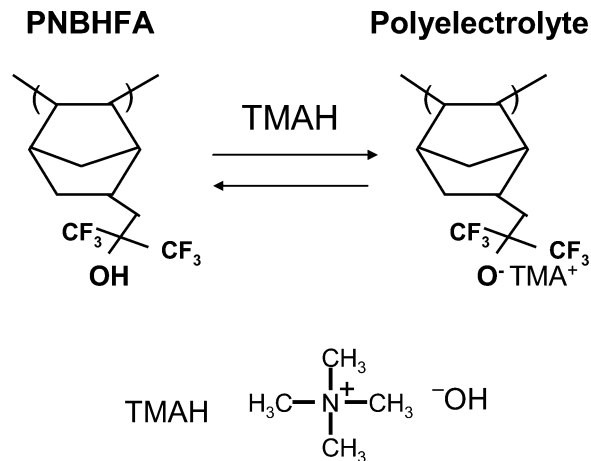
In this letter, the initial stage of polyelectrolyte dissolution is probed by measuring the electrolyte distribution within an ultrathin film (360 Å) that ionizes and swells in response to an aqueous base solution. Under the experimental conditions that we consider, the dissolution rate is greatly reduced allowing a measurement of the counterion distribution after saturation of the swelling. Specular neutron reflectivity (NR) with selectively deuterium labeled base counterions is utilized to measure the counterion distribution within this (weak polyelectrolyte) film. This is achieved by matching the scattering length density (SLD) of the solvent to the thin solid hydrogenous polymer film, thus rendering the film nearly indistinguishable from the solvent, an effect analogous to refractive index matching used in classical optics. By introducing small quantities of deuterium-labeled organic base into the solution, the enrichment within the film is observed by the enhancement of reflectivity with negligible changes in the average solution SLD. This is a zero-average contrast (ZAC) method,⁸ since we follow the distribution of deuterated-labeled counterion species in the presence of the contrast matched solvent. To complement these measurements, a full contrast (FC) method using protonated organic base in pure D₂O is used to measure the polymer profile. This approach maximizes the reflectivity contrast between the polymer and solvent.

2. Materials and Methods

[Certain equipment, instruments, or materials are identified in this paper in order to adequately specify the experimental details. Such identification does not imply recommendation by the National Institute of Standards and Technology nor does it imply the materials are necessarily the best available for the purpose.] Silicon substrates of 10.16 cm diameter and 1.27 cm thickness were prepared by an initial 5 min exposure to oxygen plasma to clean residual organic materials, followed by removal of the native oxide by immersion into a buffered oxide etch solution comprised of 10 ± 2% volume fraction HF and 5 ± 2% volume fraction NH₃F in ultrapure water for 120 ± 5 s. A controlled oxide layer was then grown in an ultraviolet/ozone chamber for 120 ± 1 s followed by priming with hexamethyldisilazane (HMDS) vapor. Poly[5-(2-trifluoromethyl-1,1,1-trifluoro-2-hydroxypropyl)-2-norbornene] (PNBHFA) ($M_{r,w} = 25\,000$, $M_{r,w}/M_{r,n} = 2.27$), chemical structure shown in Scheme 1, was filtered through a 0.45 μm poly(tetrafluoroethylene) filter (Acrodisc CR13, Pall Gelman Laboratory, Ann Arbor, MI) and spun cast onto the silicon wafers at 209 rad/s (2000 rpm) at a concentration of 2 wt %, from propylene glycol methyl ether acetate solution and postcured by baking for 15 min at 130 °C in a convection oven. The dry PNBHFA films contain 23–30% free hexafluoro-2-propanol groups that are not associated by hydrogen bonding.^{9,10}

Neutron reflectivity was performed on the NG 7 reflectometer at the NIST Center for Neutron Research. The neutron beam entered through the thick silicon wafer substrate, reflected from the polymer/liquid interface with the reflected beam traversing out through the silicon wafer. Measurements were performed in the specular reflection mode, in absolute reflected intensities (R), as a function of scattering wave vector (Q) normal to the film, $Q = 4\pi\lambda^{-1} \sin \theta$, where λ is the fixed incident neutron wavelength of 4.75 Å with resolution $\Delta Q/Q = 0.04$ (full-width half-maximum) and θ is the angle of reflection. The experimental

Scheme 1. PNBHFA Chemical Equilibrium with the Tetramethylammonium Hydroxide Base in Aqueous Solutions



reflectivity data are fit to reflectivity profiles calculated from model scattering length density profiles ($Q_c^2 = 16\pi\rho$) using the Parratt algorithm,¹¹ where ρ is the scattering length density (SLD). In general, this approach uses successive layers (a box model) of constant Q_c^2 with interface smeared by a Gaussian function leading to error function interfacial width profiles.^{12,13} For dry films, each component (silicon, silicon oxide, HMDS, and polymer) is quantitatively determined using layers of constant absorption coefficient, scattering length density, and thickness. However, for liquid and base immersed films, the polymer and base profiles are inadequately represented by one layer, so two to three layers are needed to describe the nonuniformities at the solid/solid and solid/liquid interfaces. With the Parratt algorithm, the calculated reflectivity from the trial Q_c^2 profile is fit to the experimental data using a Levenberg–Marquardt¹⁴ nonlinear least-squares method with adjustable thickness, scattering length densities, and interfacial width of the unknown layers with least-squares statistic (χ^2). Uncertainties are calculated as the estimated standard deviation from the mean. In the case where the limits are smaller than the plotted symbols, the limits are left out for clarity. For the ZAC NR experiment, a D₂O/H₂O mixture containing 0.376 volume fraction D₂O (Cambridge Isotopes, Andover MA), which contrast matches the dry polymer film Q_c^2 of $1.03 \times 10^{-4} \text{ \AA}^{-2}$, was equilibrated with the film using a liquid cell with controlled concentration of deuterium labeled d₁₂-tetramethylammonium (*d*-TMA) hydroxide (Cambridge Isotopes, Andover MA), the hydrogenated structure is shown in Scheme 1. This base counterion was chosen for convenience of a high SLD and relevance as a developer used by the microelectronics industry. Full contrast experiments used protonated TMAH in D₂O to maximize the contrast between polymer and solvent.

3. Results and Discussion

A. Neutron Reflectivity–Base Counterion Profiles. Figure 1 shows the $Q^4 \times R$ plots for ultrathin films equilibrated at different base concentrations. A very low level of reflectivity (inset), $O(10^{-5})$ beyond $Q = 0.02 \text{ \AA}^{-1}$, was observed for the film equilibrated with the pure contrast matched solvent, indicating an excellent contrast match. An enhanced reflectivity is observed for 0.00074 (pH = 10.1), 0.010, 0.0325, and 0.065 M *d*-TMA base concentrations. The shift in the fringe maxima to lower Q indicates film swelling with increased base concentration. The enhanced amplitude of reflectivity corresponds to an increased contrast between the film and solvent

(7) Dean, D.; Seog, J.; Ortiz, C.; Grodzinsky, A. *J. Langmuir* **2003**, *19* (13), 5526–5539.

(8) Benmouna, M.; Hammouda, B. *Prog. Polym. Sci.* **1997**, *22* (1), 49–92.

(9) Ito, H.; Hinsberg, W. D.; Rhodes, L.; Chang, C. *Proc. SPIE, Adv. Resist Technol. Process.* **2003**, *5039*, 70–79.

(10) Ito, H.; Truong, H. D.; Okazaki, M.; DiPietro, R. A. *J. Photopolym. Sci. Technol.* **2003**, *16* (4), 523–536.

(11) Parratt, L. *Physical Review* **1954**, *95*, 359.

(12) Ankner, J.; Majkrzak, C. *Proc. SPIE* **1992**, *1738*, 260.

(13) Russell, T. P. *Mater. Sci. Rep.* **1990**, *5*, 171.

(14) Press, W.; et al. *Numerical recipes: the art of scientific computing*; Cambridge University Press: Cambridge, U.K., 1986.

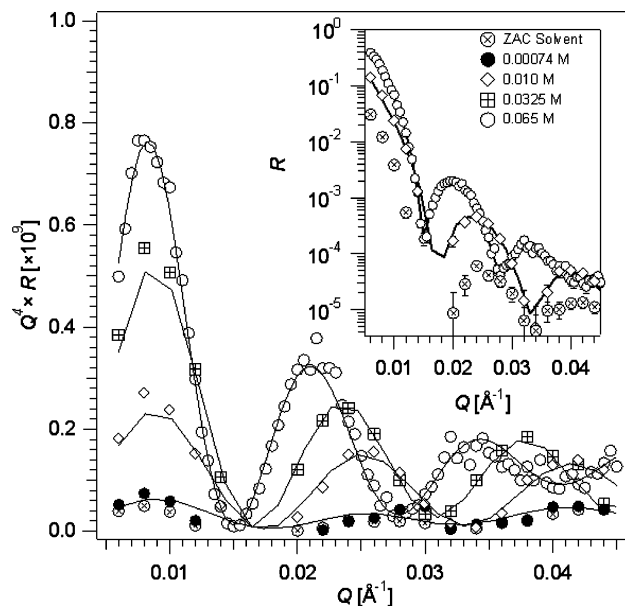


Figure 1. Enhanced reflectivity ($Q^4 \times R$) upon equilibration with increased concentrations of *d*-TMAH using contrast matched solvents. For clarity the data are shown over limited Q -range. Inset contains the absolute reflected intensities.

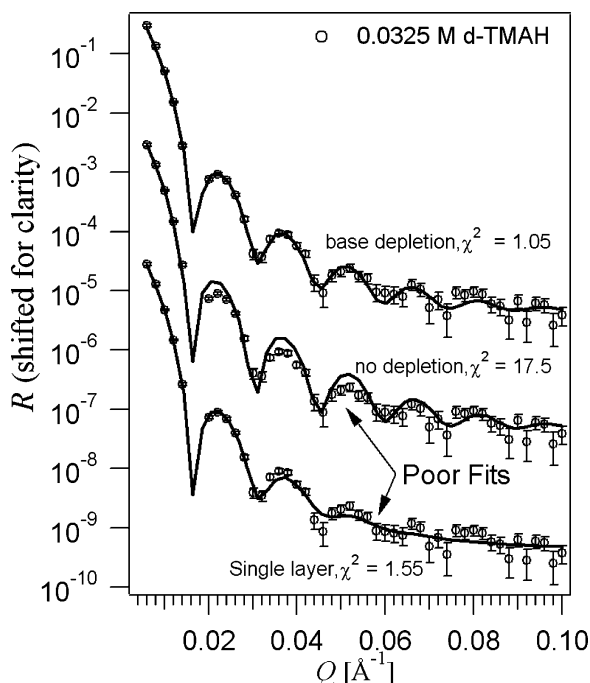


Figure 2. Fit quality with and without the substrate base-depletion layer for 0.0325 M deuterated TMAH equilibration showing entire Q -range. (Bottom) Without depletion layer a single surface layer inadequately fits fringes; (top) including substrate depletion; (middle), forced removal of depletion layer with same surface interfacial width.

arising from the penetration and condensation of deuterated TMA counterions within the film.

For thin dry films, a single layer can model the polymer layer. This is not the case for the base accumulation within the film during the *in situ* experiment as shown in Figure 2 for 0.0325 M *d*-TMAH swelling. The bottom data set is the result of modeling a single layer of absorbed base within the film with least-squares fit quality ($\chi^2 = 1.55$) resulting in a surface Q_c^2 of $1.427 \times 10^{-4} \text{ \AA}^{-2}$, a thickness of 407 Å, and a solid/liquid interfacial width of 96 Å. This approach does not represent the data as the fit quality

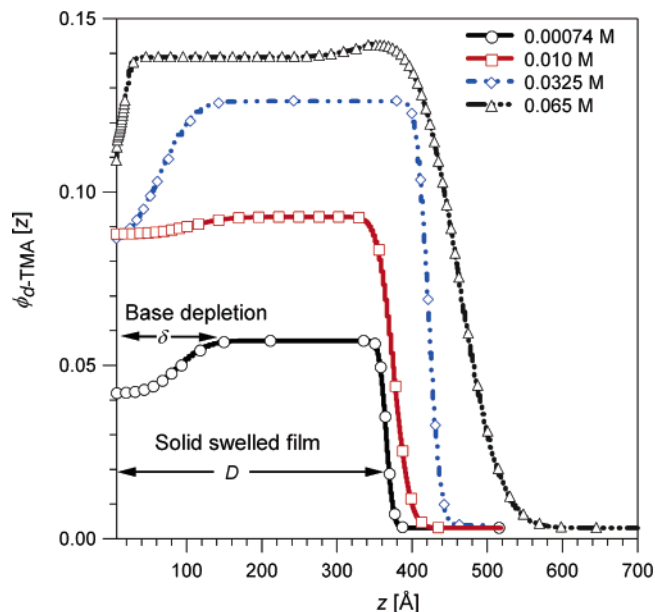


Figure 3. *d*-TMA counterion profiles within polyelectrolyte films versus distance from the silicon substrate with depleted level at the substrate and interfacial broadening at the solid/liquid interface.

degrades for $Q > 0.03 \text{ \AA}^{-1}$. Since the amplitude of reflectivity is a function of the SLD difference between the film and the contrast matched solvent and the fringe persistence is partially controlled by the interfacial width,¹³ it was suspected that a broad interface could arise at the solid substrate; hence, we implemented a second layer. The main result is shown in the topmost data set in Figure 2 in which a depletion layer near the substrate improves the statistical fit quality ($\chi^2 = 1.05$), but most notably all of the reflectivity fringes are fit with the following relevant fit parameters; a bulk Q_c^2 of $1.421 \times 10^{-4} \text{ \AA}^{-2}$ with a thickness of 355.8 Å and a depleted layer Q_c^2 of $1.289 \times 10^{-4} \text{ \AA}^{-2}$ with a thickness of 65 Å and a solid/liquid interfacial width of 29 Å. To further illustrate the importance of the depleted counterion layer, the middle data set forces the depleted layer to have equal Q_c^2 with the bulk; the difference is quite large. The fit approach always started with the single-layer, but additional layers are needed to reconcile the data.

The resultant $Q_c^2(z)$ profiles from the fits to the reflectivity data are direct measures of the *d*-TMA counterion concentration associated with the initial stages of polyelectrolyte dissolution. The *d*-TMA volume fraction, $\phi_{d\text{-TMA}}$, was calculated from $\phi_{d\text{-TMA}}(z) = (Q_c^2(z) - Q_c^2(\text{film})) / (Q_c^2(\text{p}) - Q_c^2(\text{film}))$, which is valid for a contrast matched solvent and no volume change upon mixing (additive volumes). $Q_c^2(\text{p})$ and $Q_c^2(\text{film})$ correspond to the dry and wet polymer film, respectively. The $\phi_{d\text{-TMA}}(z)$ depth profiles, presented in Figure 3, show the extent of film swelling as well as nonuniform base distribution at the substrate/polymer and the polymer/liquid interfaces. The counterion distribution within strong polyelectrolyte brushes¹⁵ demonstrated the confinement of the counterions along the nonuniform brush profile. However, in our experiments, a pH greater than the acid dissociation constant ($\text{p}K_a = 10$)^{9,20} results in increased chain segmental ionization (due

(15) Tran, Y.; Auroy, P.; Lee, L. T.; Stamm, M. *Phys. Rev. E* **1999**, *60* (6), 6984–6990.

(16) Horkay, F.; Basser, P. J. *Biomacromolecules* **2004**, *5* (1), 232–237.

(17) Houle, F. A.; Hinsberg, W. D.; Sanchez, M. I. *Macromolecules* **2002**, *35* (22), 8591–8600.

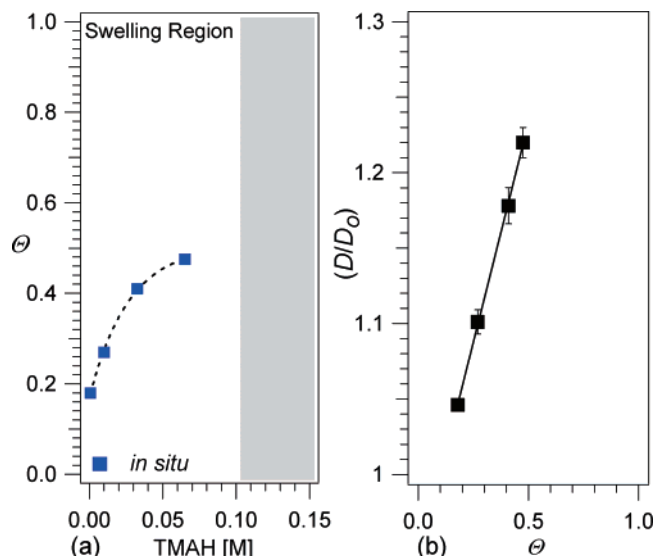


Figure 4. (a) Degree of polymer segment ionization versus base concentration illustrating the lower limit of weak polyelectrolyte ionization before dissolution occurring above 0.10 M. (b) Expansion extent dependence on the calculated degree of ionization.

to the chemical equilibrium) and decreases the Debye screening length (κ^{-1}) leading to enhanced electrostatic screening. At high degrees of ionization, the chain conformation expands from the initial dimensions, due to charge–charge repulsion between monomer segments and increased osmotic mixing pressure from the dissociated ions within the film, as found with neutralized polyelectrolyte gels.^{16,17} At the lowest base concentration (0.00074 M), the long-ranged electrostatic interactions are significant ($\kappa^{-1} = 96 \text{ \AA}$), whereas the screening length decreases to 12 \AA at 0.065 M as calculated from the bulk solution ionic strength. The role of the ionic contribution to the osmotic pressure, quantified by the base counterion concentration within the film, is an important contribution to the extent of swelling.

B. Polymer Segmental Ionization. The average polymer segmental degree of ionization (Θ) was estimated as the ratio of the number of base molecules to PNBHFA segments, $\Theta = (\phi_{d\text{-TMA}}/\phi_{\text{PNBHFA}})(\nu_{\text{PNBHFA}}/\nu_{d\text{-TMA}})$, assuming each base titrates a hexafluoroisopropanol proton; ν is the partial molar volume for the respective component and ϕ_{PNBHFA} is determined by the ratio of dry to swollen film (D_0/D), assuming additive volumes. The degree of ionization is well below 100% within the film, as shown in Figure 4a, reaching a plateau at 47% for 0.065 M; a lower bound for Θ before dissolution¹⁷ that occurs spontaneously with exposure to higher base concentration. The average ionization fraction is currently an assumed quantity in polymer photoresist material dissolution models, but many variables can affect its value.¹⁸ Figure 4b shows the linear dependence of the film expansion extent (D/D_0) versus Θ . This dependence cannot be described by either dilute solution approximations for equilibrium polyelectrolyte gels¹⁶ or a uniform chain expansion of a concentrated polyelectrolyte solution at low ionic strength.¹⁹ The source of this behavior may be due to the rod-like conformation of PNBHFA,²⁵ such that the interchain repulsion controls the expansion, rather than the conformation

as expected with flexible polyelectrolytes. Yet, the dielectric mismatch at the polymer/substrate interface may be essential to understand substrate specific effects. At the highest base concentration examined, 47% of the chain segments are ionized, yet dissolution does not proceed. The state of the film that allows for swelling, in the absence of cross-links, may be best described as the lack of a kinetic pathway to allow dissolution, perhaps a gel. Stable gels in polymer networks arise from interchain interactions due to topological effects and direct chain–chain and chain–surface associations, as well as physical cross-links. Here, we suggest that the extended hydrogen bonding and hydrophobic nature of the fluorine-containing hexafluoroisopropanol (HFA) moieties are responsible for these interactions. Observation of a fast swelling and multi-stage dissolution⁹ with PNBHFA is common. After these initial swelling stages of dissolution, the intermediate stage involves the cascading release of chains and a redistribution of the base counterion species. A measure of the true kinetics of counterion penetration is the next challenge, given our results for describing the interfacial structure.

C. Influence of Solid Substrate. The base depletion near the substrate and a broadening of the free interface of the film are unanticipated effects. The substrate/polymer interface shows a persistent depletion of base with a decreasing depletion range (δ) at higher base concentration as shown in Figure 3. The hydrophobic surface interfacial interaction is provided by the HMDS adhesion promoter with water contact angle of $72^\circ \pm 1^\circ$; however, accessible Si–OH groups can ionize under these experimental conditions. Although nonequilibrium swelling would account for this nonuniformity, the NR measurements were initiated after a saturation of the swelling, as confirmed by quartz crystal microbalance experiments. The lowest *d*-TMA concentration with a pH = 10.1, greater than the pK_a of HFA,^{9,20} show a bulk uptake of $\phi_{d\text{-TMA}} = 0.057$, yet a depletion to 0.042 occurs over the first 130 \AA . Similarly, there is a depletion in the base concentration over the first 140–145 \AA from the substrate for 0.010 and 0.0325 M solutions. In the case of the 0.010 M solution, the experiment reused the same sample from pH = 10.1 leading to a reduced depletion amount. This change in protocol led to an irreversible condensation of base within the film. Fresh samples were used throughout with this one exception. The 0.065 M solution gives rise to depletion over a shorter length scale, 32 \AA . Although the ionic radius of TMA^+ (2.9 \AA)²⁰ is larger than typical cations such as Na^+ (0.97 \AA) and K^+ (1.33 \AA) or anions Br^- (1.96 \AA) and Cl^- (1.81 \AA)^{21,22} in comparison the length scales of depletion are of longer range. We speculate that the depletion of ions near the substrate is not due to counterion size but due to electrostatics.

We can obtain some insight into this counterion depletion effect from an extension of the Debye–Hückel theory to include a plane boundary of prescribed dielectric properties by Aqua and Cornu.²² Although this mean field theory naturally leads to a depletion length on the order of κ^{-1} (the basic length of the Debye–Hückel theory) rather

(21) *Handbook of Chemistry and Physics*, 54 ed.; CRC Press: Cleveland, OH, 1974.

(22) Aqua, J. N.; Cornu, F. *J. Stat. Phys.* **2001**, *105* (1–2), 211–243.

(23) The proper characteristic scale of is $(\kappa^{-1} + b)$, hence the size (b) of the simple ion also dictates the range over which the inhomogeneous distribution heals in addition to the ionic strength.

(24) Kent, M. S. *Macromol. Rapid Commun.* **2000**, *21* (6), 243–270.

(25) Prabhu, V. M.; Wang, M. X.; Jablonski, E.; Soles, C. L.; Vogt, B. D.; Jones, R. L.; Lin, E. K.; Wu, W.-I.; Goldfarb, D. L.; Angelopoulos, M.; Ito, H. *Proceedings of the 13th International Conference on Photopolymers, Advances in Imaging Materials and Processes*, RETEC **2003**, 211–216.

(18) Flanagan, L. W.; McAdams, C. L.; Hinsberg, W. D.; Sanchez, I. C.; Willson, C. G. *Macromolecules* **1999**, *32* (16), 5337–5343.

(19) Muthukumar, M. *J. Chem. Phys.* **1996**, *105* (12), 5183–5199.

(20) Turner, J.; Soper, A.; Finney, J. *Mol. Phys.* **1990**, *70* (4), 679–700.

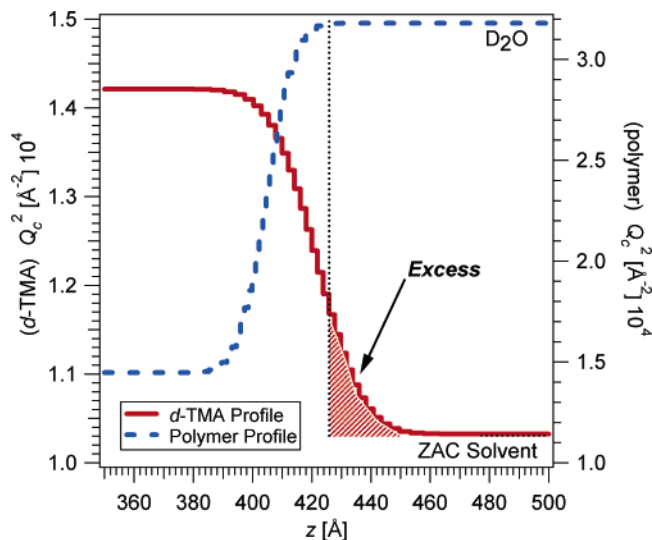


Figure 5. Excess *d*-TMA counterion at the periphery of the solid PNBHFA interface defined by a combination of zero-average and full contrast neutron reflectivity.

than the polymer radius of gyration as in our experiments, it does address the qualitative effects of how the dielectric properties of the boundary influence the counterion distribution.²³ In particular, this mean field theory²² of inhomogeneous ionic solutions predicts counterion depletion near the solid substrate when the substrate dielectric constant, relative to the solution, is less than unity, although an enhancement of the counterion concentration can occur near the surface when this dielectric ratio is greater than unity. Moreover, in the case where this ratio should be less than unity as in the present experiments, the depletion layer thickness is predicted to decrease with an increased electrolyte or base concentration. These general trends are expected to be robust for our more complex charged fluids, although the actual size of the depletion layers should more naturally reflect the size of the molecules in fluids in which interparticle interactions are larger. If these considerations are generally true, then the dielectric properties of the substrate should have a strong influence on the counterion distribution in these polyelectrolyte layers, playing a role comparable to the polymer–surface interaction in the density profiles of uncharged polymer layers.²⁴

D. Combined Polymer and Base Profiles. The polymer profile from the full contrast NR experiment is compared to the base counterion profile at the same base concentration (0.0325 M) in Figure 5. This comparison is possible due to the identical initial film thickness in the dry state and only 3 Å swelling difference in the wet state without base suggesting negligible isotopic effects. The Q_c^2 difference beyond the solid/liquid interface arises from the SLD difference between the *d*-TMAH in contrast

matched solvent versus *h*-TMAH in D₂O. The polymer/liquid interface is determined by the intersection of the terminal thickness from the full contrast NR experiment, shown as the dotted line. An excess of base is observed beyond the polymer total film thickness, overlapping the polymer profile at a base concentration of 0.0325 M. The 29 Å counterion interfacial width results from two contributions; the counterion species that are closely associated with the chain, resembling a semidilute solution and those that are unassociated, analogous to a surface excess at a charged interface. The chain segments comprising the dissolution front will require a redistribution of neutralizing counterion species during the course of dissolution. We note that our results are for the swelling of homopolymer films. The effect of copolymer structure would help generalize these results by considering the chemical mismatch between comonomer units that controls the swelling via solvent quality. These initial stage dissolution experiments highlight many possibilities for tuning variables governing the interfacial structure of dissolving polyelectrolyte layers.

4. Conclusions

Neutron reflectivity measures a nonuniform counterion profile with depletion at the substrate and an accumulation at the polymer/solution interface. Although a simple generalization of the Debye–Hückel theory to include a boundary is unable to quantitatively describe the scale of the base depletion layer, it does indicate that the dielectric mismatch between the substrate boundary and the polyelectrolyte solution should be a relevant factor in determining the counterion distribution. The decrease in the relative size of the depletion layer with an increase of base or electrolyte concentration is qualitatively consistent with this idealized model. We plan to investigate the effect of tuning the dielectric properties of the substrate in future work. We also note that a reduced accessibility of the acidic proton near the substrate, due to the extensive hydrogen bonding, may be another factor influencing the depletion effect. The solid film expansion depends linearly on the degree of ionization in these initial swelling stages of dissolution for this intrinsically stiff polymer. A full understanding of the counterion distribution in thin films will require a better understanding of ionic polyelectrolyte solutions with boundary inhomogeneities.

Acknowledgment. This work was supported by the Defense Advanced Research Projects Agency under Grant N66001-00-C-8083 and the NIST Office of Microelectronics Programs. We thank Bill Hinsberg and Frances Houle for fruitful discussions.

LA050353H